RSC Advances

COMMUNICATION

View Article Online
View Journal | View Issue

Sweet nanodot for biomedical imaging: carbon dot derived from xylitol†

Cite this: *RSC Adv.*, 2014, **4**, 23210

Daeun Kim, Yuri Choi, Eeseul Shin, Yun Kyung Jung and Byeong-Su Kim*

Received 27th February 2014
Accepted 11th April 2014

DOI: 10.1039/c4ra01723d

www.rsc.org/advances

We report a facile microwave pyrolysis approach to prepare carbon dots (CDs) using xylitol, a biomass-derived sugar alcohol. Both the surface-passivating agent (ethylenediamine) and HCl are crucial to control the luminescent properties during the synthesis of CDs. CD_{xy} exhibits bright luminescence, aqueous stability, and low cytotoxicity, and thus has high potential for biomedical applications.

Over the past two decades, semiconducting quantum dots (QDs) have received significant attention as promising nanoparticles for biological labels, electronics, and sensors due to their high photoluminescent intensity, good photostability, and tunable emission wavelength.[1] Despite these advantages, the implementation of quantum dots for biological applications is still limited due to their intrinsic toxicity and the potential environmental concerns associated with the heavy metals (*e.g.* cadmium and lead) present in QDs.[2]

Carbon nanoparticles, which are also known as carbon dots (CDs), have recently emerged as promising alternatives by virtue of their biocompatibility, low toxicity, high stability and advantageous optical characteristics, which are similar to those of QDs.[3–5] Due to their intriguing photoluminescent properties, applications of CDs are expanding into various fields, including bioimaging, biosensing, drug delivery, photocatalysis, and photovoltaics.[6] Significant research efforts have focused on producing CDs with controlled dimensions and surface properties using a variety of methods, including combustion, laser ablation, microwave pyrolysis, electrochemical oxidation, silica template synthesis, deoxygenation of natural carbon sources, and dehydration of carbohydrates.[7–10] Although this recent progress has provided efficient routes for the synthesis of CDs, the development of a simple, cost-effective, and environmentally benign method remains a challenge.

Department of Chemistry and Department of Energy Engineering, Ulsan National Institute of Science and Technology (UNIST), Ulsan 689-798, Korea. E-mail: bskim19@unist.ac.kr

† Electronic supplementary information (ESI) available: Details of synthesis and characterization, and other experimental details. See DOI: 10.1039/c4ra01723d

CDs are generally spherical in shape with diameters less than 10 nm. Moreover, CDs comprise a mixed phase of sp^2- and sp^3-hybridized carbon nanostructures in the form of conjugated carbon clusters functionalized with other surface functional groups. The photoluminescence of CDs originates from a combination of quantum confinement effects and the presence of emissive surface traps.[4] It is known that surface-passivating groups enhance the photoluminescence of CDs by increasing the number of surface defect sites.[5,9]

Many carbon precursors have been used to chemically synthesize CDs, including sugars (*e.g.* glucose, fructose, and sucrose), citric acid, and ascorbic acid. Despite their similar chemical structures, luminescent CDs cannot be easily formed from most sugar alcohols,[10–12] although some sugar alcohols have been reported to produce CDs when combined with specific inorganic ions.[12] It is highly desirable to probe the role of surface-passivating agents in the synthesis of CDs through a systematic study. In this work, we report a facile and economic approach to the synthesis of CDs by exploiting microwave-assisted pyrolysis of xylitol, which is a biomass-derived sugar alcohol. Importantly, we found that the presence of a surface-passivating agent and an additive during the synthesis are critical to controlling the photoluminescent properties of the CDs.

To synthesize the CDs, a solution of xylitol was mixed with ethylenediamine (EDA) and HCl and heated in a microwave (700 W) for 2 min (Fig. 1a). The samples are referred to as $CD_{xy}(n)$, where n represents the amount of HCl (mmol) added before microwave-assisted pyrolysis. As shown in Fig. 1b, the broad absorptions of $CD_{xy}(0)$ and $CD_{xy}(1)$ at ~230 nm represent the typical absorption of an aromatic system which is reminiscent of an sp^2 carbon network. In addition, a strong UV/vis absorption at 286 nm appears in the spectrum of $CD_{xy}(1)$, which is attributable to the n–π* transition of C=O bond, as similarly reported for other CDs.[13] A bright blue fluorescence with a maximum emission wavelength at 446 nm was observed upon excitation of $CD_{xy}(1)$ at 360 nm, whereas $CD_{xy}(0)$ did not exhibit any noticeable photoluminescence (inset in Fig. 1b). The

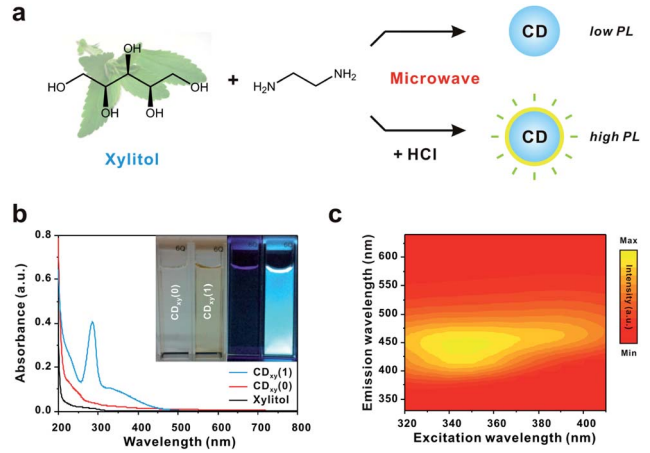

Fig. 1 (a) Schematic representation of the formation of CDs from xylitol. (b) UV/vis absorption spectra of xylitol, $CD_{xy}(0)$, and $CD_{xy}(1)$. Inset shows (left) $CD_{xy}(0)$ and (right) $CD_{xy}(1)$ solution under daylight and UV light (365 nm). (c) Two-dimensional photoluminescence spectra of $CD_{xy}(1)$ under various excitation wavelengths (320–410 nm) with 10 nm increments.

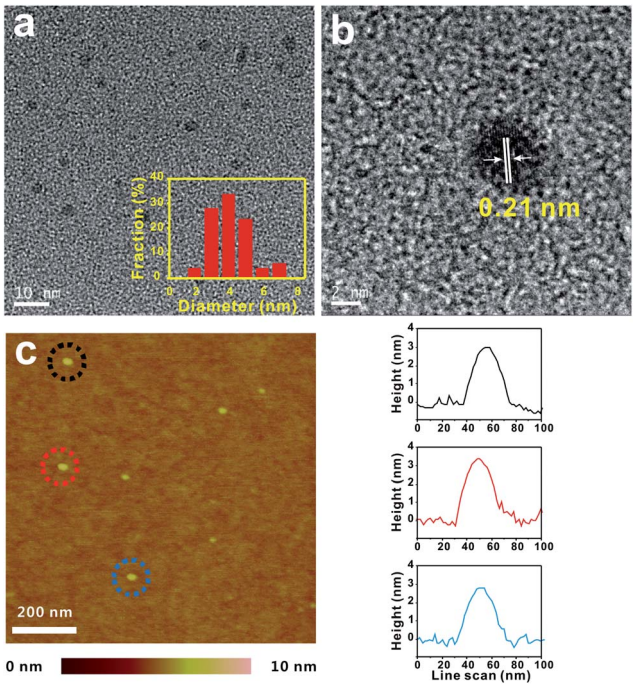

Fig. 2 (a) TEM image of $CD_{xy}(1)$ with a size distribution histogram. (b) High-resolution TEM image of $CD_{xy}(1)$. (c) Height-mode AFM image of $CD_{xy}(1)$ with line scan profiles.

quantum yield (QY) of $CD_{xy}(0)$ was determined as 0.38%, using quinine sulphate for reference. However, the addition of HCl increased the QY significantly to 7.0% for $CD_{xy}(1)$. Furthermore, this result is consistent with the exciton lifetime measured using the time-correlated single photon counting (TCSPC) technique, which yielded values of 1.75 and 2.63 ns for $CD_{xy}(0)$ and $CD_{xy}(1)$, respectively (Fig. S1, ESI†). In accordance with the previously reported excitation-dependent emission of CDs,[7,14] the maximum photoluminescence emission wavelengths of CD_{xy} are dependent on the excitation wavelength, as demonstrated in Fig. 1c. The multicolour photoluminescence arises not only from the size distribution of CD_{xy}, but also from the distribution of different emissive trap sites.[5] It is also reported that the multicolor photoluminescence of CDs is due to the heterogeneity of CDs containing chromophores at different energy levels.[15]

The size and morphology of CD_{xy} were characterized using transmission electron microscopy (TEM) and atomic force microscopy (AFM) (Fig. 2 and S2, ESI†). The TEM images reveal that the $CD_{xy}(1)$ particles are spherical with an average diameter of 4.65 ± 1.21 nm. High-resolution TEM images of $CD_{xy}(1)$ show a crystalline structure with an interlayer spacing of 0.21 nm, which corresponds to (100) lattice spacing of the graphite. The AFM image also supports the spherical morphology, with average heights of 2.53 ± 0.06 nm and 3.38 ± 0.40 nm for $CD_{xy}(0)$ and $CD_{xy}(1)$, respectively.

To further elucidate the formation mechanism of CD_{xy} in the presence of EDA and HCl additives, we characterized the samples using Fourier transform infrared (FT-IR) and high-resolution X-ray photoelectron spectroscopy (XPS). The FT-IR spectroscopy results revealed the changes in the functional groups during the course of the reaction (Fig. S3, ESI†). The FT-IR spectra of all CD_{xy} displayed characteristic peaks between 2800 and 3000 cm^{-1} (C–H stretching), broad peaks around 3300 cm^{-1} (O–H stretching), and 1000–1200 cm^{-1} (O–H bending) that imply an abundance of hydroxyl groups similar to the xylitol precursor. Moreover, the spectrum of $CD_{xy}(0)$ showed new bands at 1573 and 1417 cm^{-1}, which correspond to asymmetric and symmetric stretching vibrations of carboxylate groups. In the spectrum of $CD_{xy}(1)$, additional bands at 3154 cm^{-1} (N–H stretching), 1598 cm^{-1} (N–H in-plane), 1527 and 1464 cm^{-1} (N–H asymmetric and symmetric vibration) were observed; these clearly suggest successful surface passivation of the $CD_{xy}(1)$ with EDA. Independent of the FT-IR results, XPS was performed to further analyze the structure (Fig. S3, ESI†). Furthermore, $CD_{xy}(0)$ mainly comprises carbon, oxygen, and a small amount of nitrogen (Table S1, ESI†). It should be noted that the nitrogen content of $CD_{xy}(1)$ is 12.4%, which is higher than that in other nitrogen-doped surface-passivated CDs, while that of $CD_{xy}(0)$ is only 1.8%.[16] Accordingly, it is evident that the surface passivation reaction of CD_{xy} with EDA is significantly facilitated by the presence of HCl. Interestingly, we also found that $CD_{xy}(1)$ contains 9.4% chlorine, which suggests the formation of Cl-doped $CD_{xy}(1)$ (Fig. S4 and Table S2, ESI†); this Cl-doping likely increases the number of emissive defect sites, thus playing a critical role in enhancing photoluminescence, as well as enabling surface passivation.[17]

Due to the enhancement of CD_{xy} by the HCl additive, we further investigated the changes in the QY and zeta-potential as a function of amount of HCl added during the formation of $CD_{xy}(n)$ (typically, $n = 0$–3). Fig. 3a shows the QY curves of CD_{xy} with varying amounts of HCl added, while fixing the amount of both xylitol and EDA (1.0 mmol). Although the QY increased to 7.0% upon increasing of HCl from 0 to 1.0 mmol, the increment of the HCl additive from 1.0 to 3.0 mmol did not further

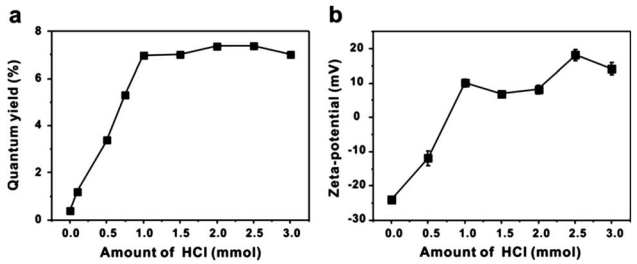

Fig. 3 (a) Quantum yield and (b) zeta-potential of CD_{xy} with varying amounts of HCl. The quantum yield was measured using quinine sulfate as a reference at an excitation wavelength of 360 nm.

improve the QY, which implies that HCl reacts with EDA and accelerates the surface-passivation reaction on CD_{xy}. Fig. 3b shows that the zeta-potentials of CD_{xy} gradually increased from -24.0 ± 0.55 mV for $CD_{xy}(0)$ to 10.0 ± 1.23 mV for $CD_{xy}(1)$; this surface charge reversal clearly suggests that the surface of CD_{xy} is passivated with amine groups derived from EDA. In other control experiments, similar phenomena were observed (Fig. S5, ESI†). The QY of CD_{xy} formed using different amounts of EDA increased up to ~7% and plateaued at over 1.0 mmol, while increasing the amounts of HCl. The zeta-potential of CD_{xy} increased from -7.10 ± 0.78 to 10.0 ± 1.23 mV with an increase of the amounts of EDA from 0 to 1.0 mmol.

Taken together, these results show that the HCl additive plays several important roles in enhancing the photoluminescence of CDs. First, H^+ ions accelerate the carbonization of carbohydrates, as was previously reported.[18] Second, H^+ ions facilitate passivation of EDA on the surface of CD_{xy}. Third, Cl^- ions can be doped onto the CD, which increases the number of emissive defect sites on CD_{xy}. Finally, to confirm the role of HCl in enhancing the photoluminescence of CDs derived from sugar alcohol, we extended our approach to other sugar alcohols, such as sorbitol (a six-carbon sugar alcohol). As expected, $CD_{sor}(1)$, which contains HCl, features bright blue luminescence and has a higher QY (5.3%) than that of $CD_{sor}(0)$ (Fig. S6, ESI†). Considering the facile preparation of CD_{xy} and its high photoluminescence and high biocompatibility owing to its origin, we investigated its potential as a biological label for living cell imaging. The cytotoxicity of $CD_{xy}(1)$ was examined using a conventional MTT assay employing two different types of cell lines: WI-38 and HeLa cells. Fig. 4a shows that $CD_{xy}(1)$ preserves an excellent cell viability of ~100% toward both cell lines up to a concentration of 0.1 mg mL^{-1}. The cell viability decreases marginally at a concentration of 1.0 mg mL^{-1}.

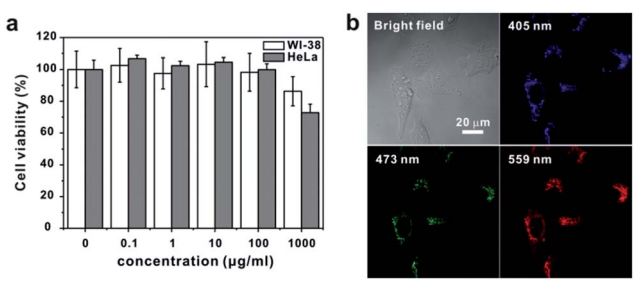

Fig. 4 (a) MTT-based cell viability assays of WI-38 and HeLa cells treated with various concentrations of $CD_{xy}(1)$. (b) Bright-field and fluorescence images of HeLa cells treated with 100 μg mL^{-1} of $CD_{xy}(1)$ for 24 h.

It is noteworthy that this concentration of $CD_{xy}(1)$ is much higher than that required for biological imaging. As a result of this superior biocompatibility, 0.1 mg mL^{-1} of $CD_{xy}(1)$ was incubated with HeLa cells for 24 h. As shown in Fig. 4b, cellular uptake of $CD_{xy}(1)$ was clearly observed, with a high fluorescence signal originating mainly from the cytoplasm and not from the cell nucleus. This result indicates that the $CD_{xy}(1)$ is easily internalized into the cell, possibly by endocytosis to the cytoplasm. Interestingly, HeLa cells incubated with $CD_{xy}(1)$ exhibit multicolor photoluminescence, *i.e.* blue, green and red, upon excitation at wavelengths of 405, 473, and 559 nm, respectively. This unique feature of CDs enables the identification of CDs during biological imaging, which is unattainable by traditional organic dyes or QDs. Moreover, laser scanning confocal fluorescence microscopy analyses indicate remarkable photostability of the CDs without any observable photobleaching.

In conclusion, we developed a simple microwave pyrolysis method to generate CDs with tunable photoluminescence from a sugar alcohol, xylitol. We demonstrated that the addition of HCl can improve the surface passivation reaction on CDs derived from sugar alcohols. Moreover, the CDs are extremely biocompatible, especially compared with semiconductor quantum dots, and thus have high potential for biomedical applications.

Acknowledgements

This work was supported by a National Research Foundation of Korea (NRF) grant funded by the Korean government (no. 2010-0028684). Y.C. and E.S. were supported by the BK21 Plus funded by the Ministry of Education, Korea (10Z20130011057).

Notes and references

1 X. Michalet, F. F. Pinaud, L. A. Bentolila, J. M. Tsay, S. Doose, J. J. Li, G. Sundaresan, A. M. Wu, S. S. Gambhir and S. Weiss, *Science*, 2005, **307**, 538; A. P. Alivisatos, *Science*, 1996, **271**, 933; I. L. Medintz, H. T. Uyeda, E. R. Goldman and H. Mattoussi, *Nat. Mater.*, 2005, **4**, 435.

2 R. Hardman, *Environ. Health Perspect.*, 2006, **114**, 165; A. M. Derfus, W. C. W. Chan and S. N. Bhatia, *Nano Lett.*, 2004, **4**, 11; J. K. Jaiswal and S. M. Simon, *Trends Cell Biol.*, 2004, **14**, 497.

3 S. J. Yu, M. W. Kang, H. C. Chang, K. M. Chen and Y. C. Yu, *J. Am. Chem. Soc.*, 2005, **127**, 17604; S. C. Ray, A. Saha, N. R. Jana and R. Sarkar, *J. Phys. Chem. C*, 2009, **113**, 18546.

4 S. N. Baker and G. A. Baker, *Angew. Chem., Int. Ed.*, 2010, **49**, 6726.

5 Y. P. Sun, B. Zhou, Y. Lin, W. Wang, K. A. S. Fernando, P. Pathak, M. J. Meziani, B. A. Harruff, X. Wang, H. F. Wang, P. J. G. Luo, H. Yang, M. E. Kose, B. L. Chen, L. M. Veca and S. Y. Xie, *J. Am. Chem. Soc.*, 2006, **128**, 7756.

6 S. J. Zhu, J. H. Zhang, C. Y. Qiao, S. J. Tang, Y. F. Li, W. J. Yuan, B. Li, L. Tian, F. Liu, R. Hu, H. N. Gao, H. T. Wei, H. Zhang, H. C. Sun and B. Yang, *Chem. Commun.*, 2011, **47**, 6858; W. J. Bai, H. Z. Zheng, Y. J. Long, X. J. Mao, M. Gao and L. Y. Zhang, *Anal. Sci.*, 2011, **27**, 243; H. Q. Tao, K. Yang, Z. Ma, J. M. Wan, Y. J. Zhang, Z. H. Kang and Z. Liu, *Small*, 2012, **8**, 281; S. J. Zhuo, M. W. Shao and S. T. Lee, *ACS Nano*, 2012, **6**, 1059; H. Choi, S. J. Ko, Y. Choi, P. Joo, T. Kim, B. R. Lee, J. W. Jung, H. J. Choi, M. Cha, J. R. Jeong, I. W. Hwang, M. H. Song, B. S. Kim and J. Y. Kim, *Nat. Photonics*, 2013, **7**, 732; H. T. Li, X. D. He, Z. H. Kang, H. Huang, Y. Liu, J. L. Liu, S. Y. Lian, C. H. A. Tsang, X. B. Yang and S. T. Lee, *Angew. Chem., Int. Ed.*, 2010, **49**, 4430.

7 H. P. Liu, T. Ye and C. D. Mao, *Angew. Chem., Int. Ed.*, 2007, **46**, 6473.

8 S. L. Hu, K. Y. Niu, J. Sun, J. Yang, N. Q. Zhao and X. W. Du, *J. Mater. Chem.*, 2009, **19**, 484; L. B. Tang, R. B. Ji, X. K. Cao, J. Y. Lin, H. X. Jiang, X. M. Li, K. S. Teng, C. M. Luk, S. J. Zeng, J. H. Hao and S. P. Lau, *ACS Nano*, 2012, **6**, 5102; L. Bao, Z. L. Zhang, Z. Q. Tian, L. Zhang, C. Liu, Y. Lin, B. P. Qi and D. W. Pang, *Adv. Mater.*, 2011, **23**, 5801; Y. X. Yang, D. Q. Wu, S. Han, P. F. Hu and R. L. Liu, *Chem. Commun.*, 2013, **49**, 4920.

9 M. J. Krysmann, A. Kelarakis, P. Dallas and E. P. Giannelis, *J. Am. Chem. Soc.*, 2012, **134**, 747.

10 H. Peng and J. Travas-Sejdic, *Chem. Mater.*, 2009, **21**, 5563.

11 H. Zhu, X. L. Wang, Y. L. Li, Z. J. Wang, F. Yang and X. R. Yang, *Chem. Commun.*, 2009, 5118; X. Y. Zhai, P. Zhang, C. J. Liu, T. Bai, W. C. Li, L. M. Dai and W. G. Liu, *Chem. Commun.*, 2012, **48**, 7955; X. F. Jia, J. Li and E. K. Wang, *Nanoscale*, 2012, **4**, 5572.

12 X. H. Wang, K. G. Qu, B. L. Xu, J. S. Ren and X. G. Qu, *J. Mater. Chem.*, 2011, **21**, 2445.

13 S. Liu, J. Q. Tian, L. Wang, Y. W. Zhang, X. Y. Qin, Y. L. Luo, A. M. Asiri, A. O. Al-Youbi and X. P. Sun, *Adv. Mater.*, 2012, **24**, 2037; X. Y. Qin, W. B. Lu, A. M. Asiri, A. O. Al-Youbi and X. P. Sun, *Catal. Sci. Technol.*, 2013, **3**, 1027.

14 A. B. Bourlinos, A. Stassinopoulos, D. Anglos, R. Zboril, M. Karakassides and E. P. Giannelis, *Small*, 2008, **4**, 455.

15 S. K. Das, Y. Y. Liu, S. Yeom, D. Y. Kim and C. I. Richards, *Nano Lett.*, 2014, **14**, 620.

16 W. B. Lu, X. Y. Qin, S. Liu, G. H. Chang, Y. W. Zhang, Y. L. Luo, A. M. Asiri, A. O. Al-Youbi and X. P. Sun, *Anal. Chem.*, 2012, **84**, 5351; C. Z. Zhu, J. F. Zhai and S. J. Dong, *Chem. Commun.*, 2012, **48**, 9367.

17 S. Hu, R. Tian, Y. Dong, J. Yang, J. Liu and Q. Chang, *Nanoscale*, 2013, **5**, 11665; Y. Q. Dong, H. C. Pang, H. B. Yang, C. X. Guo, J. W. Shao, Y. W. Chi, C. M. Li and T. Yu, *Angew. Chem., Int. Ed.*, 2013, **52**, 7800.

18 J. P. Schuhmacher, F. J. Huntjens and D. W. Vankrevelen, *Fuel*, 1960, **39**, 223.